PHYSICAL REVIEW B **94**, 100502(R) (2016)

Superfluid behavior of quasi-one-dimensional p-H_2 inside a carbon nanotube

Maurizio Rossi[1,2] and Francesco Ancilotto[3,4]
[1]*Scuola Normale Superiore, Piazza dei Cavalieri 7, I-56126 Pisa, Italy*
[2]*International Center for Theoretical Physics (ICTP), Strada Costiera 11, I-34154 Trieste, Italy*
[3]*Dipartimento di Fisica e Astronomia "Galileo Galilei" and CNISM, Università di Padova, via Marzolo 8, 35122 Padova, Italy*
[4]*CNR-IOM Democritos, via Bonomea, 265 - 34136 Trieste, Italy*
(Received 10 February 2016; revised manuscript received 21 August 2016; published 15 September 2016)

We perform *ab initio* quantum Monte Carlo simulations of para-hydrogen (p-H_2) at $T = 0$ K confined in carbon nanotubes (CNT) of different radii. The radial density profiles show a strong layering of the p-H_2 molecules which grow, with increasing number of molecules, in solid concentric cylindrical shells and eventually a central column. The central column can be considered an effective one-dimensional (1D) fluid whose properties are well captured by the Tomonaga-Luttinger liquid theory. The Luttinger parameter is explicitly computed and interestingly it shows a nonmonotonic behavior with the linear density similar to what found for pure 1D ^{3}He. Remarkably, for the central column in a (10,10) CNT, we found an ample linear density range in which the Luttinger liquid is (i) superfluid and (ii) stable against a weak disordered external potential, as the one expected inside realistic pores. This superfluid behavior could be experimentally revealed in bundles of carbon nanotubes, where deviations from classical inertial values associated with superfluid density could be measured by using quartz crystal microbalance techniques. In summary, our results suggest that p-H_2 within carbon nanotubes could be a practical and stable realization of the long sought-after, elusive superfluid phase of parahydrogen.

DOI: 10.1103/PhysRevB.94.100502

Superfluid para-hydrogen (p-H_2) represents one of the most elusive phases in nature. As liquid helium, p-H_2 is a natural candidate for displaying superfluidity by virtue of its light mass. Contrarily to helium however, it does not remains liquid down to zero temperature as a consequence of the stronger attractive interaction, which is about four times larger than the He-He one, and undergoes a crystallization transition around 14 K [1] (at saturated vapor pressure), a temperature much higher than the calculated superfluid bulk transition temperature $T \sim 1.1$ K [2]. To create superfluid p-H_2 it is therefore necessary to bring the liquid below its saturated vapor pressure curve. Attempts to produce a bulk superfluid p-H_2 sample by supercooling the normal liquid below the triple point have been unsuccessful so far [3].

As a possible way to stabilize the liquid phase of p-H_2 at low temperatures several authors have considered restricted geometries to reduce the effective attraction between molecules, and thus the zero-pressure density. For example, the lowering of the melting point compared to the bulk liquid is a well-known and rather general phenomenon in clusters [4], and a widely explored route in the search for p-H_2 superfluidity is indeed based upon the realization and study of ultrasmall p-H_2 clusters. The associated reduction of scale suggests that p-H_2 clusters could display superfluidity. This expectation is based on the fact that the smaller number of neighbors and surface effects in small clusters may hinder solidification and promote a liquidlike phase at low temperature [5]. The first prediction of superfluidity in p-H_2 clusters made of few molecules was reported in 1991 based on quantum Monte Carlo (QMC) simulations [6]. The first experimental signature of superfluidity in p-H_2 was in fact inferred from the unhindered rotation of a chromophore molecule in a cluster made of $N = 15$ p-H_2 molecules embedded in a larger ^{4}He nanodroplet [7]. Even if larger droplets of p-H_2 are found to remain liquid at low temperature [5], experiments of nonclassical rotation seem to locate the maximum size for a superfluid cluster at $N = 17$ [8]. Despite the great effort devoted to such systems [9], any attempt of a direct observation of a stable superfluid phase of p-H_2 has so far failed.

Another possibility put forward in theoretical calculations is to exploit disorder for suppressing crystallization and promote a superfluid response. However, even in the most favorable scenario, disorder gives rise to a glassy phase which is predicted to be superfluid in a metastable regime [10] but not at equilibrium [11].

Taking advantage of the understanding gained for ^{4}He systems, geometrical confinement has been considered too as a possible route to stabilize a bulk superfluid phase for p-H_2. In fact, as inferred from extensive investigations for ^{4}He in porous media such as Vycor [12], zeolites [13], and aerogel [14], as well as in superfluid films [15], quantum fluids in constrained geometries behave differently than in the bulk. Equivalent indications of possible superfluid behavior for p-H_2 in nanoconfined systems are scarce and often contradictory. A possible superfluid phase inside a (5,5) carbon nanotube was predicted by studying the equation of state of pure one-dimensional (1D) p-H_2 at $T = 0$ K with diffusion Monte Carlo [16]. However, recent path integral Monte Carlo (PIMC) calculations seem to contradict this claim, by showing that the 1D p-H_2 equilibrium phase is a crystal [17], as it also is in two-dimensional (2D) p-H_2 [18].

So far the only reported enhancement of superfluid response was obtained within PIMC simulations for p-H_2 confined inside nanocavities [19]. The confining medium discussed in this paper is however not realistic, being composed of spherical nanosized cavities coated with alkali metal thick films in order to reduce the adsorption properties of the cavity walls, which seems hardly feasible at the present time.

We follow here a different approach by addressing a more realistic system made of p-H_2 molecules in a confining system that is routinely provided by existing nanotechnologies, i.e., armchair carbon nanotubes (CNT) of different radii. Although

strictly 1D geometry precludes superfluid behavior, wider tubes where p-H_2 forms a quasi-1D system coexisting with solidlike concentric cylindrical shells could provide the ideal environment where strong evidence of the elusive superfluidity of para-hydrogen could be collected, as shown in the present work.

Our calculations are based on an exact zero temperature path integral ground state (PIGS) Monte Carlo method [20,21]. Because PIGS is a well-established computational methodology we shall not review it here. We recall only that the most relevant feature is that it provides unbiased estimates of the $T = 0$ K ground state properties directly by the microscopic Hamiltonian, by projecting in imaginary time a trial wave function. The quality of the trial wave function has the sole role to fix the length of the total imaginary time projection. Here we have considered a shadow wave function (SWF) [22], which has provided an optimal trial wave function for bulk [23], confined [24], overpressurized [25], and dimensionally reduced [26] ^{4}He systems, whose parameters have been optimized to describe p-H_2 [27]. All the approximations involved in the PIGS method, i.e., the choice of the total imaginary time τ, of the imaginary time step $\delta\tau$, and the approximation for the short imaginary time propagator, are so well controlled that the resulting systematic errors can be reduced within the unavoidable Monte Carlo statistical error making of PIGS an *exact* zero-temperature method [20,21].

In our calculations we consider N p-H_2 molecules, described as a pointlike particle with zero spin adsorbed within CNT of different radii, described by the following Hamiltonian:

$$\hat{H} = -\lambda \sum_i \nabla_i^2 + \sum_{i<j} v(|\vec{r}_i - \vec{r}_j|) + \sum_i V(\vec{r}_i), \qquad (1)$$

where $\vec{r}_i$ are the positions of the p-H_2 molecules, $\lambda = \hbar^2/2m = 12.031$ K Å^2, v describes the interaction between a pair of molecules, and V describes the interaction of a molecule with the CNT. We assume periodic boundary conditions along the tube axis. As for v, which is considered spherically symmetric, we use the well-known Silvera-Goldman potential (SG) [28]. We specifically consider three different armchair CNTs: the (10,10) CNT with radius $R = 6.80$ Å, the (12,12) CNT with radius $R = 8.19$ Å, and the (15,15) CNT with radius $R = 10.17$ Å. To model the H_2-carbon interaction we used a pair potential fitted to high level *ab initio* results on the interaction between H_2 and graphite [29]. This procedure provides a corrugated potential V, but implicitly neglects the effects of curvature, which however are found to have very little consequences for the considered CNTs [30]. By using the fourth order pair-Suzuki approximation [21] for the short imaginary time propagator we observe convergence of ground state estimates with a projection time $\tau = 0.250$ K^{-1} using a time step $\delta\tau = 1/640$ K^{-1}.

We made a number of simulations with varying number N of p-H_2 molecules from 38 up to a maximum of 432, adsorbed within the three different CNTs of increasing length $14.77 < L < 59.00$ Å. Similarly to the case of ^{4}He adsorbed in nanotubes [31–36], the p-H_2 radial density profiles $\rho_R(r)$, reported in Fig. 1, show a marked layered structure: the p-H_2 molecules form a cylindrical shell adsorbed on the inner tube

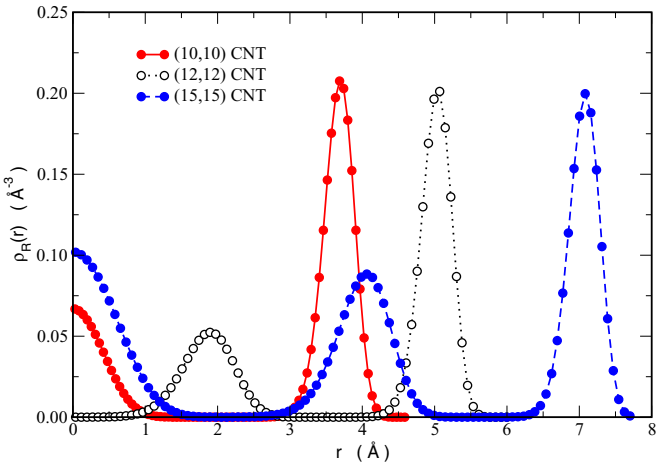

FIG. 1. Typical radial density profiles $\rho_R(r)$ for p-H_2 inside the considered CNTs. Statistical errors are smaller than the used symbols.

wall plus a central column in the (10,10) CNT, two concentric cylindrical shells in the (12,12) CNT, and two concentric cylindrical shells plus a central column in the (15,15) CNT. The promotion to the second (lower density) layer [or to the central column for the (10,10) CNT] occurs at an areal density value $\theta_P = 0.108$ Å^{-2}, which is about 15% higher than the promotion coverage to the second layer found for p-H_2 adsorbed on graphite [37]. For all the three CNT, the adsorbed layer adjacent to the tube inner surface turns out to be a crystalline two-dimensional triangular solid wrapped to form a cylinder, whose structure is incommensurate with the underlying carbon lattice. The intermediate shells [in the (12,12) and (15,15) tubes] are also a two-dimensional solid wrapped on a cylindrical surface for all the considered values of N, with no evidence whatsoever of a liquidlike behavior.

Within the PIGS method it is possible to obtain a direct estimate of the superfluid fraction ρ_s from the imaginary time diffusion of the center of mass of the system [38,39]. For the (10,10) and (12,12) CNTs, we found a sizable superfluid response, comparable with the (debated [40]) one calculated for p-H_2 embedded in a 2D Na crystal [41]. However, this large ρ_s has to be ascribed to the presence of defects in the crystalline structure of the adsorbed layer due to the mismatch between the p-H_2 lattice and the underlying carbon structure, i.e., to the actual length L of the simulated CNT. The effective ability of such defects to sustain a detectable superfluid flow [42] or rather their pinning at the structural defects in real CNTs is beyond the scope of this paper.

Our systems provide however a better candidate for superfluidity: the central column in (10,10) and (15,15) CNTs, that behaves as a quasi-1D superfluid whose properties are well captured by the Tomonaga-Luttinger liquid theory (TLL) [43–45]. The description of a confined quantum fluid by means of the TLL has been successfully applied to ^{4}He in nanopores [33,34].

TLL is a phenomenological theory that captures the low-energy properties of a wide class of quantum 1D systems with short-range interactions [43,46] in terms of two bosonic fields, $\phi(x)$ and $\theta(x)$ representing, respectively, the density and the phase fluctuations of the particle field operator

$\psi(x) = \sqrt{\rho + \partial_x \phi(x)}\, e^{i\theta(x)}$ (ρ being the average density) via the low-energy effective Hamiltonian

$$H_{\rm LL} = \frac{\hbar}{2\pi} \int dx\, (c K_L \partial_x \theta(x)^2 + \frac{c}{K_L}\, \partial_x \phi(x)^2). \qquad (2)$$

The parameter K_L (known as Luttinger parameter [47]) and the velocity c are generally independent quantities fixed by the microscopic details of the system. Such a Hamiltonian is exactly solvable, thus the knowledge of c and K_L is enough to characterize the correlation functions and the thermodynamic properties of the system. For Galilean-invariant systems, as the ones we are going to consider here, $c = \hbar\pi\rho/mK_L$ [45], thus the only parameter to be determined is K_L. Here we determine the Luttinger paramenter via QMC simulations that have largely been proven to be efficient in estimating K_L [17,48–50].

K_L governs the decay of correlations function and can be used to draw a well defined definition of (quasi)crystal and (quasi)superfluid. For $K_L < 1/2$ the static structure factor develops Bragg peaks at reciprocal lattice vectors, which is the signature of a (quasi)crystalline solid. For $K_L > 1/2$ no (quasi)diagonal long-range order is present, but the system displays a (quasi-)off-diagonal long-range order. Thus, even if no true long-range order can exist in 1D for a system of particles with short-range interaction [51], there can be a phase, known as Luttinger liquid (LL), featuring power-law decaying correlations [45], that is superfluid in the sense that it displays a quasi-off-diagonal long-range order [52,53]. Such a superfluidity manifests different degree of robustness against disorder or external potentials. Specifically, if $K_L > 3/2$ the superfluid is insensitive to a weak external disordered potential [54], while for a periodic external potential commensurate with the density with filling fraction $1/p$, the transition is located at $K_L = 2/p^2$ [53].

It was found that for narrow pores ^{4}He obeys the TLL theory with a small Luttinger parameter corresponding to solidlike character of the adsorbed phase [33,34]. On the other hand, for wider pores, the central region appears to behave like a LL but with a larger K_L indicating that the system is dominated by superfluid fluctuations, as indeed expected for superfluid ^{4}He. We will show here that a similar behavior occurs for p-H_2 in CNTs. Since the exchanges of molecules with the surrounding shells are null, the central column of p-H_2 in (10,10) and (15,15) CNT can be considered an effective one-dimensional system that can be well described via the TLL [34]. The surrounding shells have the crucial role to screen (reduce) the bare p-H_2–p-H_2 interaction, and the molecules inside the central column can be depicted as pure 1D particles (with the same mass of the initial ones) interacting via the effective potential [34]

$$v_{\rm 1D}(z) = \frac{1}{\rho_L^2} \int d^2r \int d^2r' v(\vec{r} - \vec{r}') \rho_R(r) \rho_R(r'), \qquad (3)$$

where $\vec{r} = (r,\varphi,z)$ is a vector in cylindrical coordinates and

$$\rho_L = \frac{N}{L} = 2\pi \int dr\, r \rho_R(r) \qquad (4)$$

is the linear density. The resulting effective potential is almost insensitive to the actual pore length and to the density of the central column itself. The obtained $v_{\rm 1D}$ for the (10,10) and (15,15) CNT are shown in Fig. 2, where they are also compared to the SG p-H_2–p-H_2 bare interaction potential. Notably, they can be fairly fitted by using a Lennard-Jones like formula [55]. As already observed for ^{4}He [34], the effect of the surrounding shells is that of reducing the potential well depth and of shifting the minimum to smaller separations. This can change dramatically the low-density behavior of the effective 1D system when compared to the strictly 1D p-H_2. In fact, for example, pure 1D p-H_2 is expected to display a spinodal decomposition at densities below 0.209 Å^{-1} [17], while we have been able to simulate such an effective pure 1D system down to $\rho = 0.02$ Å^{-1} without any signature of spinodal decomposition. For this pure 1D system, we have simulated $N = 50$ particles in order to minimize the finite size effects [17,50], taking $\tau = 2.50\,{\rm K}^{-1}$ and $\delta\tau = 1/320\,{\rm K}^{-1}$ to guarantee convergence to the ground state.

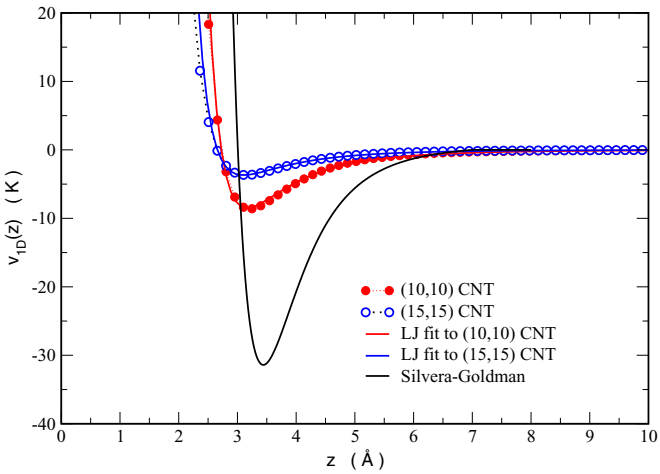

FIG. 2. Effective one-dimensional interaction potential $v_{\rm 1D}$, obtained by Eq. (3), for p-H_2 molecules in the central column inside (10,10) and (15,15) CNT. The effective potentials are compared with the Silvera-Goldman potential for the p-H_2–p-H_2 interaction. Continuous lines represent a fit of $v_{\rm 1D}$ with a Lennard-Jones (LJ) like potential.

The Luttinger parameter K_L can be extracted by the low momenta behavior of the static structure factor $S(k)$ [49,50],

$$S(k) = \frac{K_L k}{2\pi\rho}, \quad k \to 0. \qquad (5)$$

Some example of the calculated $S(k)$ for the effective 1D systems realized by the central column of p-H_2 inside the (10,10) and the (15,15) CNT are reported in Fig. 3 for different values of the linear density ρ. The linear behavior at low momenta is evident and the extracted K_L are reported in the right panel of the same figure. The dependence of K_L from the density is nonmonotonic and resembles the one for ^{3}He [49].

The key result of the present work is however that for the central column of p-H_2 inside a (10,10) CNT there is an ample density range ($0.02 < \rho < 0.08$ Å^{-1}) where $K_L > 3/2$, meaning that the LL is both superfluid and stable against the presence of a weak disordered external potential. The stability of such a 1D superfluid is crucial because p-H_2 inside the central column is expected to indeed experience an external

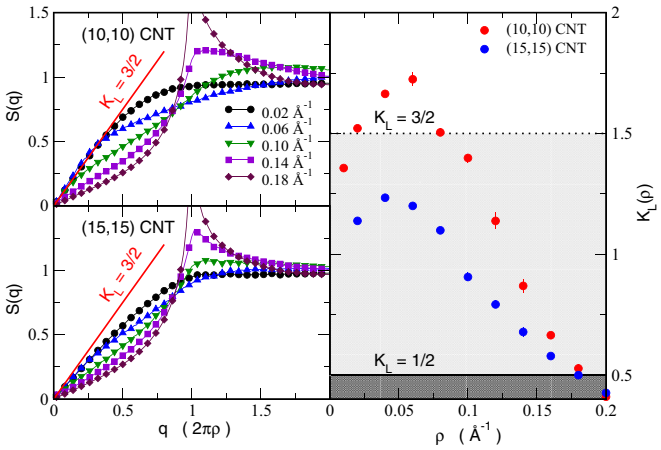

FIG. 3. Left: Static structure factors $S(q)$ for both the effective 1D systems realized by the central column of p-H_2 inside the (10,10) and the (15,15) CNT for different linear densities ρ. The momenta q are given in units of $2\pi\rho$. Error bars are smaller than the used symbols. The straight red line marks the threshold $K_L = 3/2$. Right: Luttinger parameter K_L as obtained by the low momenta behavior of the static structure factor. Both the relevant thresholds $K_L = 1/2$ [which discerns from a (quasi)crystal and a (quasi)superfluid] and $K_L = 3/2$ (which marks the stability of the superfluid against a weak disordered external potential) are also shown.

potential. For the (10,10) CNT, the potential provided by the CNT itself is practically flat on the pore axis, while the one provided by the surrounding solid layer is weak and disordered because of incommensurability effects [56]. No stable LL superfluid has been observed for the (15,15) CNT, where the K_L is always lower than 3/2. It is interesting to note that the central columns in both the CNT undergo a crystal-superfluid transition at linear densities closed to the spinodal decomposition of the pure p-H_2.

A possible way to experimentally stabilize the superfluid phase of p-H_2 is by confining it within aligned bundles of micron-sized parallel CNTs. The predicted superfluid phase of p-H_2 could be observed by using current quartz microbalance techniques [30], by measuring the frequency shifts in the shear modes of the microbalance parallel to the bundle axis. The density range where a superfluid response should be expected could be easily reached by changing the pressure (chemical potential) of the p-H_2 vapor surrounding the nanotube bundles, which determines the actual amount of fluid adsorbed inside the central columns.

While preparing this Rapid Communication, we were made aware of a recent paper where quasi-1D p-H_2 in model nanopores with smooth walls was studied by using PIMC [57] with no sign of any LL-superfluid phase. When their radius is such that the pore houses a single p-H_2 column, K_L is found to grows from the value 0.28 of the pure 1D p-H_2 [17] to values close to 1/2 but still in the (quasi)crystalline state. Even the combination of cylindrical shell plus central column has been explored in Ref. [57] for a glass pore of radius $R = 5$ Å, but with opposite results than ours. We argue that the less attractive substrate and the small radius with respect to the (10,10) CNT considered here, provide a tighter confinement for p-H_2 that strongly localizes the molecules, resulting in a Luttinger parameter even lower than the one of the pure p-H_2.

In conclusion we have studied, by using PIGS exact simulations and the TLL theory, p-H_2 within geometric confinement provided by realistic CNT of different radii. The results show the appearance, for the (10,10) and (15,15) CNTs, of a central column along the NT axis, that can be described within the TLL theory. The molecules belonging to the inner column are screened by the solid p-H_2 layers adsorbed on the surrounding CNT inner wall, resulting in pronounced quantum exchanges between molecules within the column, leading to a clear superfluid behavior in the (10,10) CNT. Our QMC simulations do indeed confirm this scenario, suggesting that p-H_2 within bundles of carbon nanotubes could be a practical realization of the elusive superfluid phase of parahydrogen.

We thank M. Boninsegni, G. Bertaina, D. E. Galli, G. Mistura, and P. L. Silvestrelli for stimulating discussions.

[1] A. C. Clark, X. Lin, and M. H. W. Chan, Phys. Rev. Lett. **97**, 245301 (2006).
[2] S. M. Apenko, Phys. Rev. B **60**, 3052 (1999); V. S. Vorob'ev and S. P. Malyshenko, J. Phys.: Condens. Matter **12**, 5071 (2000).
[3] H. J. Maris, G. M. Seidel, and T. E. Huber, J. Low Temp. Phys. **51**, 471 (1983).
[4] J. A. Alonso, *Structure and Properties of Atomic Clusters* (Imperial College Press, London, 2005).
[5] K. Kuyanov-Prozument and A. F. Vilesov, Phys. Rev. Lett. **101**, 205301 (2008).
[6] P. Sindzingre, D. M. Ceperley, and M. L. Klein, Phys. Rev. Lett. **67**, 1871 (1991).
[7] S. Grebenev, B. Sartakov, J. P. Toennies, and A. F. Vilesov, Science **289**, 1532 (2000).
[8] H. Li, R. J. Le Roy, P.-N. Roy and A. R. W. McKellar, Phys. Rev. Lett. **105**, 133401 (2010).
[9] T. Zeng and P.-N. Roy, Rep. Prog. Phys. **77**, 046601 (2014).
[10] O. N. Osychenko, R. Rota, and J. Boronat, Phys. Rev. B **85**, 224513 (2012).
[11] J. Turnbull and M. Boninsegni, Phys. Rev. B **78**, 144509 (2008).
[12] G. M. Zassenhaus and J. D. Reppy, Phys. Rev. Lett. **83**, 4800 (1999).
[13] R. Toda, M. Hieda, T. Matsushita, N. Wada, J. Taniguchi, H. Ikegami, S. Inagaki, and Y. Fukushima, Phys. Rev. Lett. **99**, 255301 (2007).
[14] J. Yoon, D. Sergatskov, J. Ma, N. Mulders, and M. H. W. Chan, Phys. Rev. Lett. **80**, 1461 (1998).
[15] J. Nyeki, R. Ray, B. Cowan, and J. Saunders, Phys. Rev. Lett. **81**, 152 (1998), and references therein.
[16] M. C. Gordillo, J. Boronat, and J. Casulleras, Phys. Rev. Lett. **85**, 2348 (2000).
[17] M. Boninsegni, Phys. Rev. Lett. **111**, 235303 (2013).
[18] M. Boninsegni, Phys. Rev. B **70**, 193411 (2004).

[19] T. Omiyinka and M. Boninsegni, Phys. Rev. B **90**, 064511 (2014).
[20] A. Sarsa, K. E. Schmidt, and W. R. Magro, J. Chem. Phys. **113**, 1366 (2000).
[21] M. Rossi, M. Nava, L. Reatto, and D. E. Galli, J. Chem. Phys. **131**, 154108 (2009).
[22] S. Vitiello, K. Runge, and M. H. Kalos, Phys. Rev. Lett. **60**, 1970 (1988).
[23] D. E. Galli and L. Reatto, Mol. Phys. **101**, 1697 (2003).
[24] M. Rossi, L. Reatto, and D. E. Galli, J. Low Temp. Phys. **168**, 235 (2012).
[25] M. Rossi, E. Vitali, L. Reatto, and D. E. Galli, Phys. Rev. B **85**, 014525 (2012).
[26] E. Vitali, M. Rossi, F. Tramonto, D. E. Galli, and L. Reatto, Phys. Rev. B **77**, 180505(R) (2008).
[27] F. Operetto and F. Pederiva, Phys. Rev. B **69**, 024203 (2004).
[28] I. S. Silvera and V. V. Goldman, J. Chem. Phys. **69**, 4209 (1978).
[29] D. Y. Sun, J. W. Liu, X. G. Gong, and Z-F. Liu, Phys. Rev. B **75**, 075424 (2007).
[30] See Supplemental Material at http://link.aps.org/supplemental/10.1103/PhysRevB.94.100502 for details on the p-H_2–CNT interaction potential V, the curvature effects, and more details on the possible experimental setup.
[31] M. Rossi, D. E. Galli, and L. Reatto, Phys. Rev. B **72**, 064516 (2005).
[32] M. Rossi, D. E. Galli, and L. Reatto, J. Low Temp. Phys. **146**, 95 (2007).
[33] A. Del Maestro, M. Boninsegni, and I. Affleck, Phys. Rev. Lett. **106**, 105303 (2011).
[34] A. Del Maestro, Int. J. Mod. Phys. B **26**, 1244002 (2012).
[35] B. Kulchytskyy, G. Gervais, and A. Del Maestro, Phys. Rev. B **88**, 064512 (2013).
[36] L. Pollet and A. B. Kuklov, Phys. Rev. Lett. **113**, 045301 (2014).
[37] L. W. Bruch, M. W. Cole, and E. Zaremba, *Physical Adsorption: Forces and Phenomena* (Oxford University Press, Oxford, 1997).
[38] S. Zhang, N. Kawashima, J. Carlson, and J. E. Gubernatis, Phys. Rev. Lett. **74**, 1500 (1995).
[39] M. Nava, D. E. Galli, M. W. Cole, and L. Reatto, Phys. Rev. B **86**, 174509 (2012).
[40] M. Boninsegni, Phys. Rev. B **93**, 054507 (2016).
[41] C. Cazorla and J. Boronat, Phys. Rev. B **88**, 224501 (2013).
[42] M. Rossi, E. Vitali, D. E. Galli, and L. Reatto, J. Phys.: Condens. Matter **22**, 145401 (2010)
[43] S.-I. Tomonaga, Prog. Theor. Phys. **5**, 544 (1950).
[44] J. M. Luttinger, J. Math. Phys. **4**, 1154 (1963).
[45] F. D. M. Haldane, Phys. Rev. Lett. **47**, 1840 (1981).
[46] T. Giamarchi, *Quantum Physics in One Dimension* (Oxford University Press, New York, 2003).
[47] Two predominant definitions of the Luttinger parameter K_L exist in the literature. The one used here is the inverse of the one employed in Refs. [17,33–35].
[48] A. Del Maestro and I. Affleck, Phys. Rev. B **82**, 060515(R) (2010).
[49] G. E. Astrakharchik and J. Boronat, Phys. Rev. B **90**, 235439 (2014).
[50] G. Bertaina, M. Motta, M. Rossi, E. Vitali, and D. E. Galli, Phys. Rev. Lett. **116**, 135302 (2016).
[51] N. D. Mermin and H. Wagner, Phys. Rev. Lett. **17**, 1133 (1966).
[52] T. Eggel, M. A. Cazalilla, and M. Oshikawa, Phys. Rev. Lett. **107**, 275302 (2011).
[53] M. A. Cazalilla, R. Citro, T. Giamarchi, E. Orignac, and M. Rigol, Rev. Mod. Phys. **83**, 1405 (2011).
[54] T. Giamarchi and H. J. Schulz, Europhys. Lett. **3**, 1287 (1987); **37**, 325 (1988).
[55] We have fit our v_{1D} with the formula $v_{LJ}(z) = 4\varepsilon[(\frac{\sigma}{z})^m - (\frac{\sigma}{z})^{m/2}]$ obtaining $\varepsilon = 8.485$ K, $\sigma = 2.726$ Å, and $m = 9.230$ for the (10, 10) CNT and $\varepsilon = 3.683$ K, $\sigma = 2.658$ Å, and $m = 8.957$ for the (15, 15) one.
[56] The external potential experienced by the p-H_2 molecules in the central column is the sum of the potential due to the CNT itself and the one due to the adsorbed layer. The CNT produces a periodic potential whose maximum excursion in energy (i.e., the energy difference between top and hollow site adsorption energies) are of the order of 0.03 K, i.e., 10^{-3} times the SG well and 4×10^{-3} times the v_{1D} well. The adsorbed layer produces a potential which is disordered due to the presence of defects induced by incommensurability, whose maximum excursion in energy in 0.3 K, i.e., 10^{-2} times the SG well and 4×10^{-2} times the v_{1D} well.
[57] T. Omiyinka and M. Boninsegni, Phys. Rev. B **93**, 104501 (2016).